Statistical analysis of the Deep-seated Gravitational Slope Deformation ability of influencing landslide spatial distribution

M. Capitani *[a], A. Ribolini [a], P.R. Federici [a]

[a] *Department of Earth Sciences, University of Pisa, Via S. Maria 53, 56126 Pisa (Italy)*
* *Corresponding author. E-mail address: capitani@dst.unipi.it; phone +390502215845*

Abstract

An attempt to analyze the Deep-seated Gravitational Slope Deformation (DSGSD) ability of influencing the landslide spatial distribution was carried out in the Milia basins, Tuscany, Italy. Detailed geomorphological mapping, combined with the analysis of aerial photography, enabled us to build two landslide inventories using a time scale. The landslides related to a period before 1975 were used to create the statistical models, while those related to a period after 1975 were used to validate the models predictive power. Geology, slope angle, slope aspect, distance to hydrographic elements and distance to tectonic lineaments were considered in the analysis as landslide-predisposing factors. In order to quantify the importance of the DSGSD as landslide-influencing factor, the DSGSD-presence-absence map was introduced in the statistical analysis using a stepwise process. More specifically, the inventory landslide maps and the landslide-related factor maps were processed using a conditional analysis applied to all the possible factor combinations, producing landslide susceptibility maps with five susceptibility classes. The comparison between the distribution of the post-1975 landslides and that derived from models provided the predictive power of each factor combination, which in turn has been used to evaluate the DSGSD ability of influencing the landslide spatial distribution.

Keywords Deep-seated Gravitational Slope Deformation, Landslide susceptibility, MSUE-Conditional Analysis Method, Predictive power, Central Italy.

1. Introduction

Deep-seated Gravitational Slope Deformations (DSGSDs) (Dramis and Sorriso-Valvo, 1994) affect large mountain slope areas worldwide modifying the morphological characteristics of the slope itself (Bovis and Evans, 1996; Julian and Anthony, 1996; Kinakin and Stead, 2005) as well as the fracture system of the involved lithotypes (Agliardi et al., 2001; Bachmann et al., 2009; Pánek et al., 2011a). All the slope modifications relating to the formation of DSGSD and its evolution could play a non-negligible role as landslide-predisposing factors. More specifically, DSGSD could be an important predisposing factor for the slope evolution in landsliding processes. However, the link between landslides and DSGSD has not been clearly shown (Bovis and Evans, 1996; Bisci et al., 1996; Sorriso-Valvo et al., 1999), although many landslides have occurred in rock mass obviously affected by DSGSDs (Crosta, 1996; Agliardi et al., 2009a,b; Kellerer-Pirklbauer et al., 2010; Pánek et al., 2011a,b). Over the last few decades, many different analysis methods have been applied to study the gravitational evolution of DSGSDs (Boukharov and Chanda, 1995; Crosta and Agliardi, 2003; Bachmann et al., 2004, 2006; Stead et al., 2006; Jomard et al., 2007). However, results remained restricted to a relatively short time period of observations (several years) and to homogeneous or only slightly heterogeneous slopes (El Bedoui et al., 2009).

In order to give some clues about the importance of DSGSD as landslide-influencing factor, in this study a statistical analysis approach has been applied to Unique Condition Units (UCUs) (Carrara et al., 1995). More specifically, a Landslide Susceptibility (LS) analysis has been performed in a Central-Tuscany basin where DSGSDs have strictly conditioned the landscape geomorphological evolution. The LS analysis has been carried out first not considering DSGSD as a landslide-influencing factor and then introducing the DSGSD as independent variable. This procedure has been used to evaluate if the introduction of DSGSD into the analysis could imply a likelihood degree improvement of the LS best model, with an appreciable statistical significant level.

In this study, the conditional analysis method has been chosen among the methods of statistical analysis used to create LS maps, because it appears to be one of the easiest to understand and to read for non-specialists (Carrara et al., 1995; Chung et al., 1995). Moreover, the conditional analysis method applied to factor combinations has fewer limitations than other systems of statistical analysis (Clerici et al., 2006, 2010). More specifically, the bivariate analysis and the logistic regression analysis need independence variables (Cliff and Ord, 1981; Dey et al., 2000; Neuhäuser and Terhorst, 2007), while discriminant analysis requires normal distribution of the covariates (Hosmer and Lemeshow, 1999; Giudici, 2005; Härdle and Simar, 2007).

In order to achieve the study goal rigorously, it was also considered necessary to perform the LS analysis using two landslide inventories relating to a period preceding and succeeding a fixed date (Chung and Fabbri, 2008; Guzzetti et al., 2006; Blahut et al., 2010; von Ruette et al., 2011). More detailed, the model validation procedure was based on the “wait and see” concept (Chung and Fabbri, 1999), for which, in the spatial database, it was assumed that the time of the study was the year 1975 and that all the spatial data available in 1975 were compiled, including the distribution of the landslides which occurred prior to that year. Consequently, the landslides relating to a period before 1975 were used to create the models, while those relating to a period later than 1975 were used to validate the models predictive power.

2. Study area

The study area is the Milia basin (Fig. 1), which has an extension of 101 km^2 and an elevation ranging from 39 m to 913 m above sea level, with an average of 336 m (standard deviation = 167.5 m). The basin is stretched out in a SW direction and shows a prevalent hilly character. Approximately 80% of the study area is located between the altitude of 503.5 m and the minimum value that characterizes the basin in the corresponding closing section. Only near the eastern side of the Milia basin, where the morphological-structural highland of Poggione Mountain occurs, the altitude values tend to increase until the maximum of 913 m. Most of the streams of higher order (Strahler, 1952) have a general anti-apenninic management type and show strong, vertical erosion tendencies in the north-eastern part of the basin. In the western sector, the river action evolves into prevalent lateral erosion.

2.1. Main geological and geomorphological features

In the Milia basin the compressional events occurring before and during the collisional Apennine episode originated the complex sheet stack where the Ligurian and Sub-Ligurian units are emplaced above the Tuscan Domain (Costantini et al., 2000, 2002) (Fig. 1). All of these allochthonous units are characteristic of distal turbiditic and hemipelagic environments and are composed by altering siltitic, argillitic and fine arenitic formations and by argillitic with inter-bedded limestone formations. Tuscany units are represented prevalently by the Mesozoic carbonate succession, associated with very few outcrops of the cretaceous-tertiary turbiditic and hemipelagic sequence. Tuscany units are over-thrusted above the Monticiano-Roccastrada Unit, which represents the outcrop of the Tuscany “Autochthon” Metamorphic Unit. The Monticiano-Roccastrada Unit outcrops with very limited extension only in the eastern part of the basin and it is characterized by alternating phyllites and marbles. Neogene-Quaternary formations, representative of continental and coastal-marine environments, are characterized by sandy clays and sandy conglomerates deposits.

All tectonic units are characterized by a complex deformation history related to the pre and post collisional events. Post collisional deformations are strictly related to the extensional tectonic, which began at the end of the Early Miocene and caused the partial collapse of the Apennines (Carmignani et al., 1994). The Pleistocene tectonic evolution was followed by a rapid sinking of the hydrographic network. The lowering of the hydrographic network is suggested by numerous fluvial terraces located at different altitudes along the basin.

The morphology of the study area is also strongly conditioned by the numerous mass movements related to prevalent translational slide, rotational slide and flow types (Cruden and Varnes, 1996). DSGSDs are also present (Fig. 1) and their evolution appears strictly related to the Pleistocene tectonic evolution and the base level fluvial lowering. These morphologies are very similar in their type to those described by several authors (e.g., Zischinsky, 1966; Agliardi et al., 2001; Agliardi et al., 2009a,b). In particular, in the Milia basin, DSGSDs are characterized by sizes comparable to the whole slope, displacements relatively small in comparison to the slope itself and by evident morphological features as doubled ridges, scarps, counterscarps, trenches and toe bulging. For each of these phenomena, deformation can be consider as a large oblique “sagging” along deep, maybe confined, sliding surface. In this regard, the scarps and the counterscarps that affect the DSGSDs of the studied basin could be considered as surface expressions of those downslope- and upslope-dipping shear surfaces which have been observed in many previous works (Agliardi et al., 2001; Agliardi et al., 2009a,b; Bachmann et al., 2009; El Bedoui et al., 2009;). Overall, 23 DSGSDs affected the Milia basin each one extending between 0.2 km^2 and 1.2 km^2, whereas the total area involved in DSGSD is about 6.2 km^2 (6.1% of the study area). About 87% of DSGSDs occurs in the Ligurian units, with a DSGSD density up to 16%, while 13% of DSGSD area involves Neogene-Quaternary formations (density over 8%). All the DSGSDs of the Milia basin are involved in landsliding processes.

3. Methods: Basic theory, database building and procedures for LS zonation

3.1. The MSUE-Conditional Analysis Method

The conditional analysis method applied to factor combinations (Clerici et al., 2002) is based on Bayes' Theorem (Morgan, 1968), which states that the probability of occurrence of an event A conditioned by the occurrence of an event B is determined as the ratio between the probability of the simultaneous occurrence of the two events [$P(A \cap B)$] and the probability of the occurrence of the conditioning event [$P(B)$]. In LS assessment the conditional probability of landslide occurrence is defined by computing the landslide density in correspondence with different combinations of the landslide-predisposing factors (conditioning events) (Carrara et al., 1995). More specifically, the method considers a number of environmental factors, which are thought to be strictly connected with landslide occurrence. The data layers in which each factor is subdivided into classes are crossed in order to obtain all the possible factor combinations (UCU-maps). For each of these factor combinations the landslide density is then quantified within each UCU by crossing the relative UCU-map with the landslides chosen as model training dataset. Considering that landslide density is assumed to be equivalent to the future landslide probability at a specific UCU (Carrara et al., 1995), from this process we obtain a number of LS models which is equal to the number of the possible factor combinations. Afterwards, the best model is chosen by comparing the distribution of landslides used as validation dataset and those derived from the models.

This method tends to assess which factor combination is more suitable to define the LS zonation with the greatest predictive ability.

Since all statistical methods are based on the common assumption that landslides will be more likely to occur in areas where boundary conditions are similar to areas where landslides have occurred (Carrara et al., 1995), they necessarily require the knowledge of the factor conditions existing before the landslide occurrence. In this study, apart from the landslides used as model validation dataset, the available geo-environmental factor maps represent the post landsliding situation. Therefore, for the landslides used as model training dataset it was necessary to carry out the factor conditions existing before landsliding. In similar studies it was agreed on that the pre-landslide conditions may be similar to those found in an external neighborhood of the landslide source area (Süzen and Doyuran, 2004; Clerici et al., 2006, 2010; Havenith et al., 2006a, b; Nefeslioglu et al., 2008; Vergari et al., 2011).

In this study the landslides have been identified by their Main Scarps Upper Edges (MSUEs, Clerici 2006), because they allow for easier automatic research of the factor values in the undisturbed belt external to the rupture zone of the landslide (Clerici et al., 2006; 2010). In order to consider the UCUs present in the external neighborhood of the landslide source area an upstream buffer of 20 m is used for each MSUE. Therefore the method applied to the LS zonation of the Milia basin assumes the conditional probability of landslide occurrence for a given UCU as the ratio between the sum of each area of that UCU which falls within the MSUE buffer and its total area.

3.2. Landslide dataset

The landslide map is the result of the two-year (2009-2010) geological and geomorphological field survey carried out in the framework of a regional project “CIPE/Regione Toscana: Carta Geologica Regione Toscana e geo-tematiche derivate” (www.regione.toscana.it). Field survey was carried out using the Tuscany Region topographic maps (at the scale 1:10.000) and the Tuscany Region orthophotos (1-m ground sample distance ortho imagery rectified to a horizontal accuracy of within ±4 m) dating back to 1975 and 2006, respectively.

Geomorphological field survey was also carried out with the aid of the stereoscopic interpretation of 1975 aerial photographs (flight EIRA75) and GPS point acquisition (Garmin 60CSx; accuracy ≤ 3m, precision ≤ 1m).

The landslides of the Milia basin were split into two temporal groups with the aid of the stereoscopic analysis of the aerial photographs relating to 1975. The landslides occurred before 1975 have been used as model training set, while the landslides occurred after 1975 have been used as model validation set. In accordance to Guzzetti et al. (1999), LS analysis should be carried out for different landslide types. For this reason, the landslides were grouped into separate datasets based on their movement typology. Moreover, following the division proposed by Keefer (1984), only deep-seated (≥ 3m) landslides were considered to avoid the introduction of shallow and easily degradable landslides into the model validation dataset.

In the Milia basin a total of 2,039 landslides were identified. The landslides cover a surface of about 22.6 km^2, representing 22.4% of the whole study area. Based on the observations during field work these 2,039 landslides were divided into three typologies: translational slide (1,577), flow (155), and rotational slide (307). Among these, 128 translational slides, 31 flow and 46 rotational slides have occurred after 1975.

Overall, the Milia basin is affected mainly by translational slide-type landslides. Since the aim of this study was to analyze the DSGSD ability of influencing the landslide spatial distribution using a statistical approach, only these translational slides are used for the analysis because this assures that the predictive model can be adequately trained due to their abundance.

The MSUEs relative to the training and validation dataset were carried out from the geomorphological map previously digitized in ArcGIS. Afterwards, the maps depicting the buffers were carried out from the MSUE maps using Buffer tool of ArcInfo 9.2 (ESRI).

3.3. Instability factors

In the scientific literature, many factors are considered predisposing landslide occurrence (Soeters and Van Westen, 1996; van Westen et al., 2008). Considering that among the landslide-predisposing factors usually used in the LS assessment, with high benefit value / cost, lithology, slope angle and slope aspect are the most common

(Rodriguez et al., 2008; Nefeslioglu et al., 2008; Rotigliano et al., 2012), and that the evolution of the study basin is strictly connected to the Pliocene-Pleistocene tectonic activity as well as to the fluvial erosion phases, in this study, lithology, slope angle, slope aspect, distance to hydrographic elements and to tectonic lineaments have been considered as predisposing factors. Moreover, for the purpose of this study, DSGSD has additionally been introduced to the LS analysis as a possible landslide-inducing factor.

The factor maps relating to lithology as well as to distance from hydrographic elements and from tectonic lineaments, have been derived from the geological map performed for the "CIPE" Tuscany project. For lithology, different classes have been extracted from geological map on the basis of their lithological and structural analogies (Fig. 2). Furthermore, considering that in the study areas many landslides have occurred from the body of precedent landslides, it was also necessary to insert the landslide body into a specific class. The maps related to the distance from hydrographic elements and from tectonic lineaments have been carried out subjecting the relative linear feature-class to a process of buffering with the construction of four distance classes based on percentile criteria.

By exploiting the 3D Analyst and Spatial Analyst extensions of ArcInfo 9.2 the slope angle and the slope aspect maps have been derived from the 5×5 m^2 pixel resolution DEM, obtained by transforming a TIN into a GRID. The TIN was generated by the interpolation of digital contour lines and elevation points extracted from the Tuscany Region topographic maps (scale 1:10.000) dating back to 1975. Slope angle has been reclassified into six classes with similar areas (percentile criteria), while slope aspect has been reclassified into the eight most frequently adopted classes corresponding to the angular sectors, 45° wide and clockwise from north (equal interval criteria).

The DSGSD-presence-absence map was carried out from the geomorphological map of the "CIPE" Tuscany project. The free-landslide slope affected by DSGSD and the free-landslide slope not affected by DSGSD were digitalized in a polygonal vector format and codified with a respective unique value (1, DSGSD-presence; 0, DSGSD-absence).

The class extension for each factor and their relative MSUE density are showed in the table 1.

3.4. Selection of the best model

A Python program in the Model-Builder of ArcInfo has been created, in which all the geoprocessing steps necessary for the model builds and their validation have been automatized. In the Python script all the possible combinations of landslide-related factors (UCU maps) are initially computed. The UCU maps are then intersected with the buffer maps of the MSUEs belonging to the pre-1975 dataset. For each UCU the ratio of the sum of the UCU area that falls within the MSUE buffer and the total area for that UCU is calculated. Afterwards, the UCUs are grouped into five density classes (LS classes) on the basis of their ratio value (UCU density). For the class definition a similar method already applied by Clerici et al. (2010) is used. The classes are defined on the basis of the MSUE mean density (If, prior probability) carried out by dividing the total MSUE buffer area by the basin area. This value is the middle point of the middle class. More precisely, the class interval on which LS maps are created is Ci= (If/5)×2 and the susceptibility class intervals are: 0-Ci (Very Low), Ci-2Ci (Low), 2Ci-3Ci (Medium), 3Ci-4Ci (High) and 4Ci-5Ci (Very High). For each of the possible combinations of the landslide-related factors, the LS models have been built.

The validation procedure has been performed in the Model-Builder to choose the best model. Considering that the validation procedure is based on the "wait and see" concept, the distribution of the pre-1975 MSUEs (training set) is compared with that of the post-1975 MSUEs (validation set). More specifically, for each LS class the absolute value of the difference between the pre-1975 and post-1975 MSUE percentage is computed. The sum of the latter values, the Validation Error (VE), is reported for each LS model. The VE assesses the predictive power of each model built and its value ranging from 0 (the best predictive power) to 200 (the worst predictive power).

According to Clerici et al. (2010), a good validation is a necessary but not a sufficient prerequisite for assessing the model efficiency. A good model should have a great dispersion around the landslide mean density value to distinguish between significantly different landslide density conditions. Therefore the mean deviation (MD) of the UCU density has been computed for each model and the ratio MD/VE (Best Model Index, BMI) has been utilized to choose the best LS model, which should have the highest BMI value.

3.5. Statistical significance of the best model

In order to define how the predictive ability of the best model actually represents the maximum likelihood between the landslide groups used for the model construction and validation, an analysis of the reduced chi-square (χ^2) was performed.

The χ^2 value for a model defines the probability of finding a likelihood between the observed and the expected probability of a certain event A, which is better than that defined by the model itself (Pugh and Winslow, 1966, Kendall and Stuart, 1979; Buccianti et al., 2003). Considering that the forecasting model should be made using an older landslide inventory, and more recent landslides should be used for the evaluation of the prediction (Chung and Fabbri, 1999, 2008; Guzzetti et al., 2006; Blahut et al., 2010; von Ruette et al., 2011), for each model the percentage of landslides belonging to the validation group that fall into a susceptibility class must be necessarily considered as expected value of the landsliding probability in that class.

Therefore, in this study the chi-square value is calculated from:

$$\chi^2 = \frac{1}{4}\sum_{i=1}^{5} \frac{[(\%\ \text{MSUE buffer area pre} - 75)i - (\%\ \text{MSUE buffer area post} - 75)i]^2}{(\%\ \text{MSUE buffer area post} - 75)i}$$

4. Results and discussion

4.1. The best LS model

The LS analysis of the Milia basin initially has been performed without considering DSGSD as landslide-influencing factor (case I) and then introducing the DSGSD as independent variable (case II). For both cases the 10 models with the highest BMI are shown in the table 2. The best model for each case is related to the model factor combination (MFC) that characterizes the table first row.

For case I, the Lithology-Slope angle factor combination (LS) represents the best model with a BMI = 8,238.3 and VE = 5.2. The error is prevalently concentrated in correspondence of the medium (class 3) and high (class 4) susceptibility classes, where the model tends to overestimate and underestimate respectively the landslide probability occurrence (Fig. 3). In fact, in these two classes we have approximately 76% of the overall validation error, with a sum of respective absolute errors (│ (% landslide area Post-75) - (% landslide area Pre-75) │) that reaches the value of 3.9%. In the medium susceptibility class the relative error (% landslide area Post-75 - % landslide area Pre-75) assumes a value of 1.6%, while in the high susceptibility class it has a negative value equal to - 2.4%.

The best model relating to the case II is characterized by the Lithology-Slope angle-DSGSD factor combination (LSDs) and it shows the lowest validation error (VE = 3.7) among all those created for both cases. The error is concentrated in correspondence with the medium (class 3) and very high (class 5) susceptibility classes, where the model tends to lightly overestimate and underestimate respectively the probability of landsliding (Fig. 3). In these two classes, we have approximately 75% of the overall validation error, with a sum of absolute errors that reaches the value of 2.8%. In the medium susceptibility class the relative error assumes a value of 1.47%, while in the very high susceptibility class it has a negative value equal to - 1.31%. Finally the model shows a good capacity in the differentiation of the landslide density (MD = 4,297) between the various classes. This is also visible from the comparison of the areas that characterize the susceptibility classes for which we have statistically significant extensions. The medium-class has an extension of 19.7 km^2, strictly comparable to that of the extreme classes that have values of about 29.3 km^2 (class 1) and 24.5 km^2 (class 5).

Overall, in the Milia LS analysis, the introduction of the DSGSD-presence-absence map has given us an improvement of the best model VE which moves from 5.2 (case I) to 3.7 (case II) with a VE reduction of 28.8%. Therefore, in the Milia basin, lithology, slope angle and DSGSD-presence-absence maps gave more satisfactory results as landslide-predicting factors. More than 60% of the slope area affected by DSGSD is characterized by LS greater than that *a priori* (Fig. 4a).

In the best LS-model the comparison between the slope conditions (UCUs) affected by DSGSD and those non-affected by DSGSD gives us some clues about how the translational slide distribution in the Milia basin has been conditioned by DSGSD. In DSGSD-free areas, translational slide susceptibility map outlines hillslope sections where both ligurian and gravelly (Pleistocene) formations outcrop as very prone to landslides, with a slope angle above 12° and 10°, respectively (Table 3). In slopes affected by DSGSDs, the very-high translational slide susceptibility zone is concentrated in shale and marly limestone within slope angle interval of]20-90°] and of]15-20°], respectively, while in gravelly formations the very-high translational slide susceptibility zone is located within slope angle intervals of]12-15°] and]20-90°]. By comparing the LS of the lithology-slope angle UCUs that are affected and non-affected by DSGSDs (Fig. 4b), it is possible to note how DSGSD has lightly acted over ligurian formations as a slope-stabilizing geo-environmental factor. Only for the gravelly formations with slope angle values between]4-10°] we assist to an increasing of the LS, which moves from medium-susceptibility class (areas non-affected by DSGSD) to high-susceptibility class (areas affected by DSGSD) (Table 3).

This different effects of the DSGSDs on different lithotypes is not surprising considering that ligurian units are strongly tectonically anisotropic with several different-axial fold, joint and fault populations. The LS decrease observed for these formations could be related to all structural modifications that occur during DSGSD evolution (Bachmann et al., 2009, El Bedoui et al., 2009; Pánek et al., 2011a,b), which could facilitate a deeper water circulation and a predisposition of deeper landslides (Delgado et al., 2011), i.e., rotational slides. Conversely, in the gravelly formations, which outcrop with a generally sub-horizontal stratification, the development of DSGSD-fracture systems may facilitate translational sliding processes in basin sectors without very steep slopes.

4.2. Statistical significance of the best model-VE improvement

The improvement of the best model VE implies that for the translational slide-type landslides of the Milia basin, DSGSD has probably played a non-negligible role as landsliding-predisposing factor. On the other hand the following questions occur: In which degree is the improvement of the model power prediction statistically significant? And in which degree is the assertion statistically significant, that the DSGSDs have conditioned the spatial distribution of the translational slide-type landslides in the Milia basin? In order to answer to these questions an analysis of the reduced chi-square (χ^2) was performed (Table 4).

Considering that all the best models have been created with the same number of degrees-of-freedom (number of classes of susceptibility - 1), the analysis of χ^2 allows us to compare the predictive capabilities of each of these models. In fact, regardless of how the territory was divided and reclassified into five classes of susceptibility, the likelihood degree of the models is always calculated on the same χ^2 probability distribution curve (integral function of Pugh and Winslow, 1966), which is related to systems with four degrees-of-freedom.

The obtained values were compared to the probability table of χ^2 with four degrees-of-freedom (Pugh and Winslow, 1966; Buccianti et al., 2003), and the probabilities P($\chi^2 < \chi^2$ observed.) have been determined for each of the two-case best models (Table 4).

From the model likelihood chi-square test it is possible to see that, if we consider a *p*-value of P($\chi^2 < \chi^2$ observed.) < 0.05, both models can be considered as the best. Contrariwise, if we consider a *p*-value of P($\chi^2 < \chi^2$ observed) < 0.01, only the model that includes the DSGSD factor can be considered as the best. Considering that the two-case best models are different only for the presence/absence of the DSGSD factor, the improvement of the model likelihood chi-square can be attributed to the introduction of the DSGSD factor only. More specifically, the introduction of the DSGSD factor in the statistical analysis has made it possible to maximize the likelihood degree of the best model until a high level of statistical significance. In other words, the assertion that in the Milia basin the DSGSDs have conditioned the spatial distribution of the translational slide-type landslides can be accepted at the 99 percent level.

Considering that we have used a conditional analysis method applied to UCUs, the improvement of the model likelihood chi-square from the best model of the case I to that of the case II appears highly relevant. In fact, the conditional analysis method applied to UCUs presents some limitations regarding the introduction in the analysis itself of small UCUs. The introduction in the conditional analysis of UCUs of small size can reduce the predictive ability of the statistical models (Carrara et al., 1995; Guzzetti et al., 1999; Clerici et al., 2010). The UCUs creating process can lead to a quantity of terrain units equal to the product between the class numbers of the environmental factors included in the analysis. Consequently, the probability of creating a considerable number of small UCUs rises according to the increase in both the number of factors and their class number subdivisions. Although the introduction of the DSGSD factor map in the best model of the case I redoubles the possibility of creating small UCUs in relation to that derived from the factor combination of this last model, it has implied a likelihood degree improvement of the resulting LS model. Therefore, for the Milia basin we have convincing evidences that DSGSD is a significant landslide-predisposing factor.

5. Conclusion

The general aim of this work was to highlight some considerations that could be useful to understand the role played by DSGSD in influencing the landslide distribution. Over the last few decades many multidisciplinary investigations have been carried out in order to resolve the link between DSGSDs and landslides. In this study, the DSGSD importance as landslide-influencing factor has been investigated from a statistical point of view. In order to achieve the study goal, the conditional analysis method has been applied to a basin where DSGSDs affect large slope sectors.

The analysis results, which are strictly related to the statistical link between DSGSDs and translational slides, lead us to assume that the DSGSD acts as a very important landslide-distribution conditioning factor. More specifically, the introduction of the DSGSD factor in the statistical analysis has made it possible to maximize the likelihood degree of the LS best model, until a high level of statistical significance (99%).

In the studied basin, DSGSD has different influences on different lithotypes. In shale and marly-limestone formations, DSGSD has lightly promoted the slope stability, while in basin-sectors where gravelly formations crop out in addition to generally not very steep slopes DSGSD has acted as landslide-inducing factor.

Overall, for translational slide-type landslides, this study stresses that DSGSDs should be included into statistical analysis to enhance the predictive power of the LS models, especially in basins where large portions of the slopes are involved in such phenomena.

However, the statistical link between DSGSDs and other landslide typologies still remains unresolved and it should be studied in future works as well as the DSGSD effects on lithotypes different from those considered in this study.

Acknowledgments

This research was supported by the Tuscany Region Project "*CIPE/Regione Toscana: Carta Geologica Regione Toscana e geo-tematiche derivate*" (www.regione.toscana.it), in which the authors are involved. The authors would like to thank Prof. A. Clerici and two anonymous reviewers for their helpful comments and suggestions that improved the paper. The authors are also grateful to the Editor-in-Chief Prof. Takashi Oguchi for his recommendations. We thank R. A. Riedler (University of Vienna) for the improvement of the English text.

References

Agliardi, F., Crosta, G., Zanchi, A., 2001. Structural constraints on deep seated slope deformation kinematics. Engineering Geology 59, 83–102.

Agliardi, F., Crosta, G.B., Zanchi, A., Ravazzi, C., 2009a. Onset and timing of deep-seated gravitational slope deformations in the eastern Alps, Italy. Geomorphology 103, 113–129.

Agliardi, F., Zanchi, A., Crosta, G.B., 2009b. Tectonic vs. gravitational morphostructures in the central Eastern Alps (Italy): constraints on the recent evolution of the mountain range. Tectonophysics 474, 250–270.

Bachmann, D., Bouissou, S., Chemenda, A., 2004. Influence of weathering and preexisting large scale fractures on gravitational slope failure: insights from 3-D physical modelling. Natural Hazards and Earth Sciences 4, 711–717.

Bachmann, D., Bouissou, S., Chemenda, A., 2006. Influence of large scale topography on gravitational rock mass movements: new insights from physical modelling. Geophysical Research 33, 1–4.

Bachmann, D., Bouissou, S., Chemenda, A., 2009. Analysis of massif fracturing during Deep-Seated Gravitational Slope Deformation by physical and numerical modeling. Geomorphology 103, 130–135.

Bisci, C., Burattini, F., Dramis, F., Leoperdi, S., Pontoni, F., Pontoni, F., 1996. The Sant'Agata Feltria landslide (Marche Region, central Italy): a case of recurrent earth flow evolving from a deep-seated gravitational slope deformation. Geomorphology 15, 351–361.

Blahut, J., van Westen, C.J., Sterlacchini, S., 2010. Analysis of landslide inventories for accurate prediction of debris-flow source areas. Geomorphology 119, 36–51.

Boukharov, G.N., Chanda, M.W., 1995. The three processes of brittle crystalline rock creep. International Journal of Rock Mechanics and Mining Science 32, 325–335.

Bovis, M.J., Evans, S.G., 1996. Extensive deformations of rock slopes in southern Coast Mountains, southwest British Columbia, Canada. Engineering Geology 44, 163–182.

Buccianti, A., Rosso, F., Vlacci, F., 2003. Metodi matematici e statistici nelle scienze della terra. Vol., 3. Tecniche statistiche. Liguori, Napoli.

Carmignani, L., Decandia, F.A., Fantozzi, P., Lazzarotto, A., Liotta, D., Meccheri, M., 1994. Tertiary extensional tectonics in Tuscany (Northern Apennines, Italy). Tectonophysics 238, 295-315.

Carrara, A., Cardinali, M., Guzzetti, F., Reichenbach, P., 1995. GIS technology in mapping landslide hazard. In: Carrara A, Guzzetti F, (Eds.). Geographical Information Systems in Assessing Natural Hazards. Kluwer Academic Publisher, Dordrecht, pp. 135–175.

Chung, C.F., Fabbri, A.G., Van Westen, C.J., 1995. Multivariate regression analysis for landslide hazard zonation. In: Carrara, A., Guzzetti, F. (Eds.), Geographic Information Systems in Assessing Natural Hazards. Kluwer Academic Publishers, Netherlands, pp. 107–133.

Chung, C.F., Fabbri, A.G., 1999. Probabilistic prediction models for landslide hazard mapping. Photogramm Eng Remote Sensing 65, 1389–1399.

Chung, C.F., Fabbri, A.G., 2008. Predicting landslides for risk analysis—spatial models tested by a cross-validation procedure. Geomorphology 94, 438–452.

Clerici, A., Perego, S., Tellini, C., Vescovi, P., 2002. A procedure for landslide susceptibility zonation by the conditional analysis method. Geomorphology 48, 349–364.

Clerici, A., Perego, S., Tellini, C., Vescovi, P., 2006. A GIS-based automated procedure for landslide susceptibility mapping by the conditional analysis method: the Baganza valley case study (Italian Northern Apennines). Environ. Geol. 50, 941–961.

Clerici, A., Perego, S., Tellini, C., Vescovi, P., 2010. Landslide failure and runout susceptibility in the upper T. Ceno valley (Northern Apennines, Italy). Nat. Hazards 52, 1-29.

Cliff, A.D., Ord, J.K., 1981. Spatial Processes: Models and Applications. Pion, London.

Costantini, A, Lazzarotto, A., Liotta, D., Mazzanti, R., Mazzei, R., Salvatorini, G., 2000. Note illustrative della Carta Geologica d'Italia alla scala 1:50.000, Foglio 306 – Massa Marittima. Servizio Geologico d'Italia.

Costantini, A, Lazzarotto, A., Mazzanti, R., Mazzei, R., Salvatorini, G., Sandrelli, F., 2002. Note illustrative della Carta Geologica d'Italia alla scala 1:50.000, Foglio 285 – Volterra. Servizio Geologico d'Italia.

Cruden, D.M., Varnes, D.J., 1996. Landslide types and processes. In: Turner AK, Schuster RL (Eds.) Landslides investigation and mitigation, Special Report 247, Transportation Research Board, National Research Council, Washington, pp. 36–75.

Crosta, G.B.,1996. Landslide, spreading, deep seated gravitational deformation: analysis, examples, problems and proposals. Geogr. Fis. Din. Quat. 19, 297–313.

Crosta, G.B., Agliardi, F., 2003. Failure forecast for large rock slides by surface displacement measurements. Canadian Geotechnical Journal 40, 176–191.

Delgado, J., Vicente, F., García-Tortosa, F., Alfaro, P., Estévez, A., Lopez-Sanchez, J.M., Tomás, R., Mallorquí, J.J., 2011. A deep seated compound rotational rock slide and rock spread in SE Spain: Structural control and DInSAR monitoring. Geomorphology doi:10.1016/j.geomorph.2011.02.019.

Dey, K.D., Ghosh, K.S., Mallick, K.B., 2000. Generalized Linear Model; a Bayesian Perspective. Marcel Dekker, New York.

Dramis, F., Sorriso-Valvo, M., 1994. Deep seated slope deformations, related landslide and tectonics. Engineering Geology 38, 231–243.

El Bedoui, S., Guglielmi, Y., Lebourg, T., Jean-Louis Pérez, J., 2009. Deep-seated failure propagation in a fractured rock slope over 10,000 years: The La Clapière slope, the south-eastern French Alps. Geomorphology 105, 232-238.

Giudici, P., 2005. Data Mining: metodi informatici, statistici e applicazioni. McGraw-Hill, Milano.

Guzzetti, F., Carrara, A., Cardinali, M., Reichenbach, P., 1999. Landslide hazard evaluation: a review of current techniques and their application in a multi-scale study, Central Italy. Geomorphology 31, 181–216.

Guzzetti, F., Reichenbach, P., Ardizzone, F., Cardinali, M., Galli, M., 2006. Estimating the quality of landslide susceptibility models. Geomorphology 81, 166–184.

Havenith, H.B., Strom, A., Caceres, F., Pirard, E., 2006a. Analysis of landslide susceptibility in the Suusamyr region, Tien Shan: statistical and geotechnical approach. Landslides 3, 39–50.

Havenith, H.B., Torgoev, I., Meleshko, A., Alioshin, Y., Torgoev, A., Danneels, G., 2006b. Landslides in the Mailuu-Suu Valley, Kyrgyzstan—hazards and impacts. Landslides 3, 137–147.

Härdle, W., Simar, L., 2007. Applied Multivariate Statistical Analysis. Springer, New York.

Hosmer, D.W., Lemeshow, S., 1999. Applied Survial Analysis. John Wiley and Song, New York.

Julian, M., Anthony, E., 1996. Aspects of landslide activity in the Mercantour Massif and the French Riviera, southeastern France. Geomorphology 15, 275–289.

Jomard, H., Lebourg, T., Tric, E., 2007. Identification of the gravitational boundary in weathered gneiss by geophysical survey: La Clapière landslide (France). Journal of Applied Geophysics 62, 47–57.

Keefer, D.K., 1984. Landslides caused by earthquakes. Geological Society of American Bulletin 95, 406–421.

Kellerer-Pirklbauer, A., Proske, H., Strasser, V., 2010. Paraglacial slope adjustment since the end of the Last Glacial Maximum and its long-lasting effects on secondary mass wasting processes: Hauser Kaibling, Austria. Geomorphology 120, 65–76.

Kendall, M., Stuart, A., 1979. The Advanced Theory of Statistics: Inference and Relationship. Griffin, London.

Kinakin, D., Stead, D., 2005. Analysis of the distributions of stress in natural ridges forms: implications for the deformation mechanisms of rock slopes and the formation of sacking. Geomorphology 65, 85–100.

Morgan, B.W., 1968. An introduction to Bayesian statistical decision process. Prentice-Hall, New York.

Nefeslioglu, H.A., Duman, T.Y., Durmaz, S., 2008. Landslide susceptibility mapping for a part of tectonic Kelkit Valley (Eastern Black Sea region of Turkey). Geomorphology 94, 401–418.

Neuhäuser, B., Terhorst, B., 2007. Landslide susceptibility assessment using “weights of evidence” applied to a study area at the Jurassic escarpment (SW-Germany). Geomorphology 86, 12-24.

Pánek, T., Tábořík, P., Klimeš, J., Komárková, V, Hradecký, J., Šťastný, M., 2011a. Deep-seated gravitational slope deformations in the highest parts of the Czech Flysch Carpathians: Evolutionary model based on kinematic analysis, electrical imaging and trenching. Geomorphology doi:10.1016/j.geomorph.2011.01.016.

Pánek, T., Šilhán, K., Tábořík, P., Hradecký, J., Smolková, V., Lenart, J., Brázdil, R., Kašičková, L., Pazdur A., 2011b. Catastrophic slope failure and its origins: Case of the May 2010 Girová Mountain long-runout rockslide (Czech Republic). Geomorphology 130, 352–364.

Pugh, E.M., Winslow, G.H., 1966. The analysis of physical measurements. Addison-Wesley, London.

Rodríguez, G.M.J., Malpica, J.A., Benito, B., Díaz, M., 2008. Susceptibility assessment of earthquake-triggered landslides in El Salvador using logistic regression. Geomorphology 95, 172–191.

Rotigliano, E., Cappadonia, C., Conoscenti, C., Costanzo, D., Agnesi, V., 2012. Slope units-based flow susceptibility model: using validation tests to select controlling factors. Nat. Hazards 61, 143–153.

Soeters, R., van Westen, C.J., 1996. Slope instability recognition, analysis, and zonation. In: Turner AK, Schuster R L, (Eds.) Landslides investigation and mitigation, Special Report 247, Transportation Research Board, National Research Council, Washington, pp. 129–177.

Sorriso-Valvo, M., Gullà, G., Antronico, A., Tansi, C., Amelio, M., 1999. Mass-movement, geologic structure and morphologic evolution of the Pizzotto–Greci slope (Calabria, Italy). Geomorphology 30, 147–163.

Stead, D., Eberhardt, E., Coggan, J.S., 2006. Developments in the characterization of complex rock slope deformation and failure using numerical modelling techniques. Engineering Geology 83, 217–235.

Strahler, A.N., 1952. Quantitative geomorphology of erosional landscape. C.R. 19th Intern. Geol. Cong. Algiers. Sect 13, part 3, 341-354.

Süzen, M.L., Doyuran, V., 2004. Data-driven bivariate landslide susceptibility assessment using geographical information systems: a method and application to Asarsuyu catchment, Turkey. Engineering Geology 71, 303–321.

van Westen, C.J., Castellanos, E., Kuriakose, S.L., 2008. Spatial data for landslide susceptibility, hazard, and vulnerability assessment: an overview. Engineering Geology 102, 112–131.

Vergari, F., Della Seta, M., Del Monte, M., Fredi, P., Lupia Palmieri, E., 2011. Landslide susceptibility assessment in the Upper Orcia Valley (Southern Tuscany, Italy) through conditional analysis: a contribution to the unbiased selection of causal factors. Nat. Hazards Earth Syst. Sci., 11, 1475–1497.

Von Ruette, J., Papritz, A., Lehamann, P., Rickli, C., Or, D., 2011. Spatial statistical modeling of shallow landslides – Validating predictions for different landslide inventories and rainfall events. Geomorphology 133, 11-22.

Zischinsky, U., 1969. Uber Sackungen. Rock Mechanics 1, 30–52.

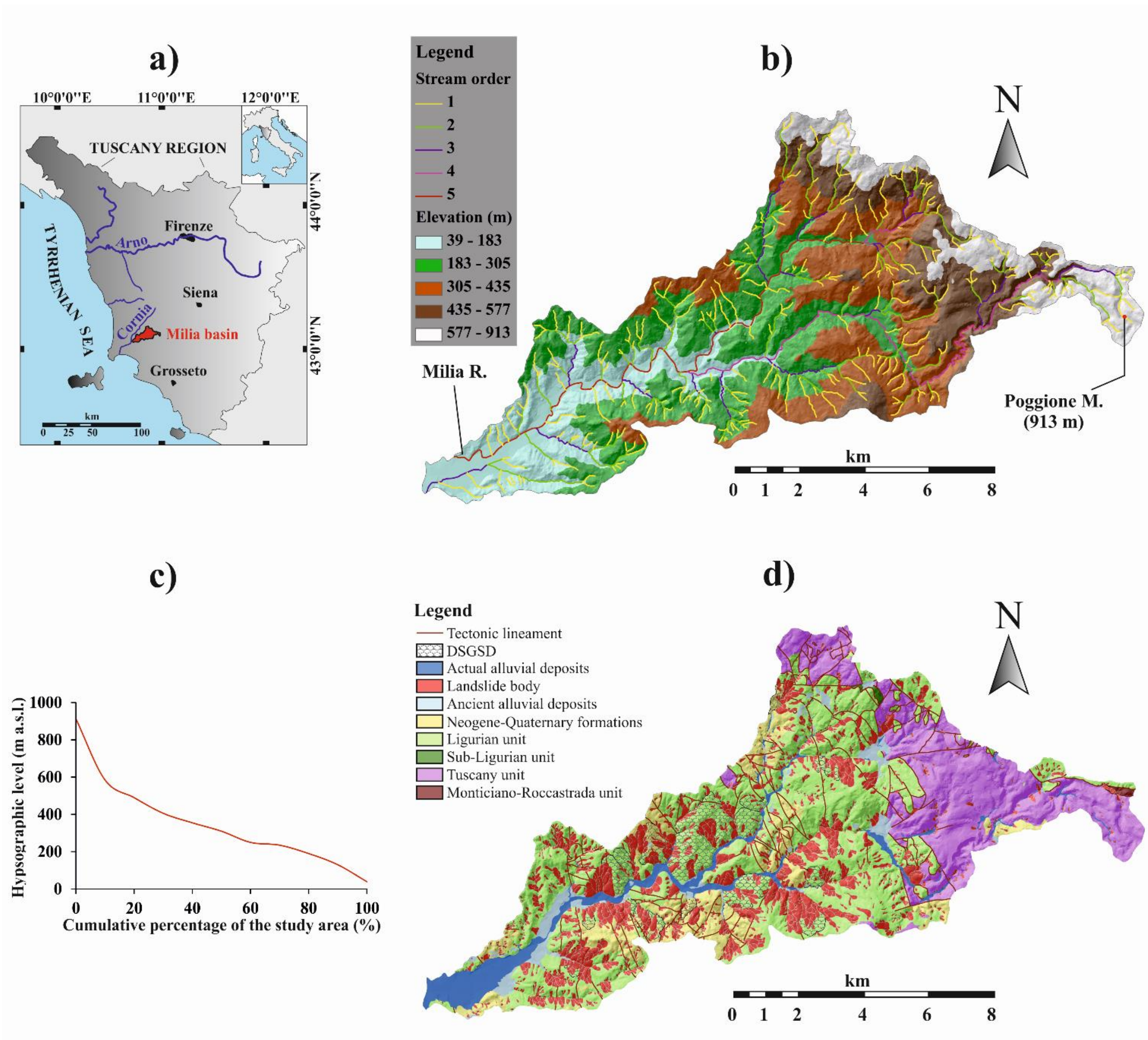

Fig. 1. Location of the study area (a) and its hydrographic (b), hypsographic (c) and geological (d) characteristics. The hydrographic elements are ordered according to Strahler (1952).

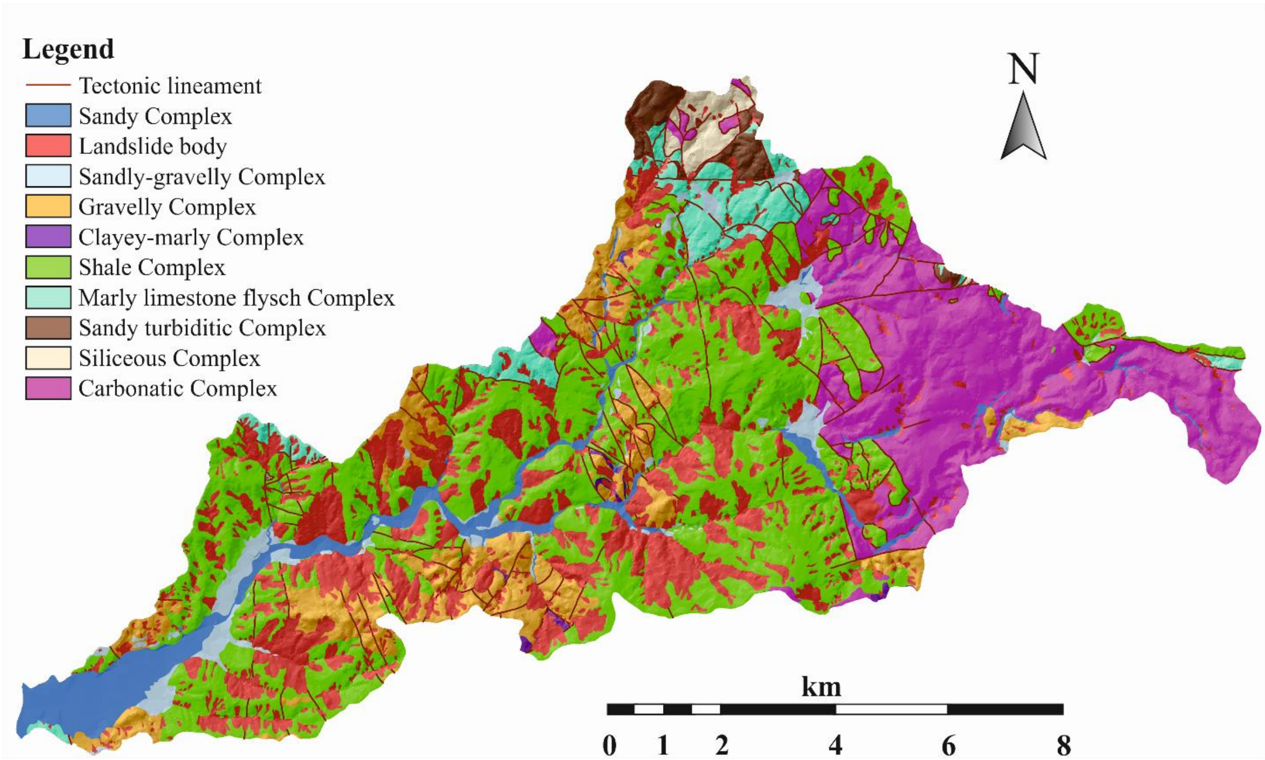

Fig. 2. Lithological factor map of the studied basin.

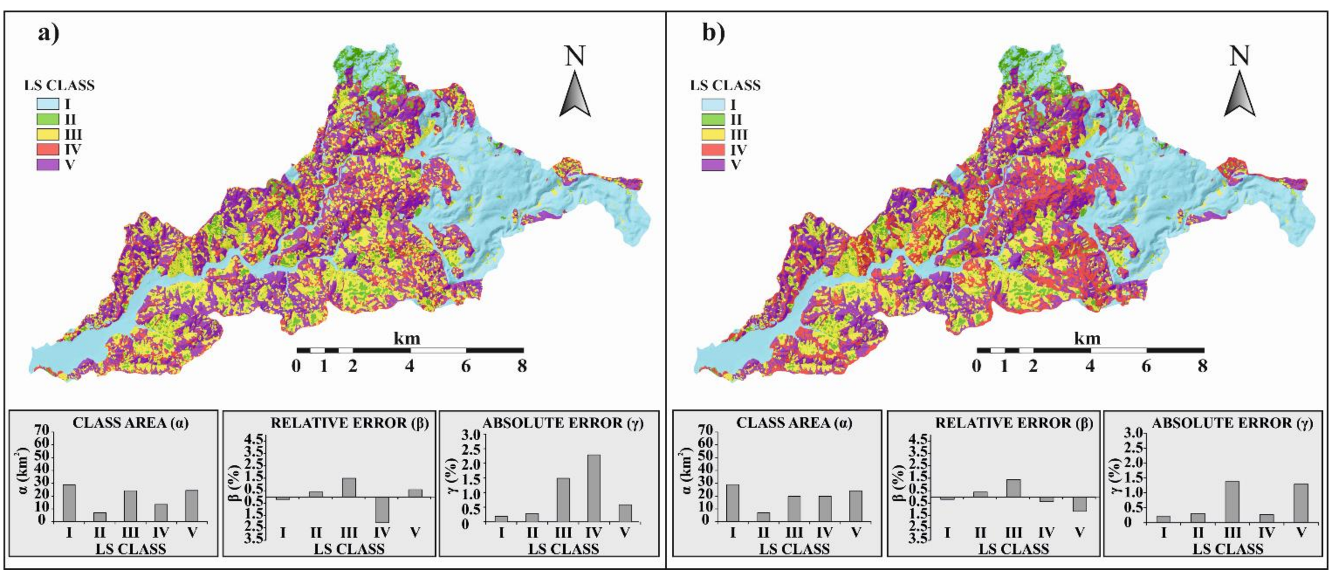

Fig. 3. The best model for the case I (a) and for the case II (b). Landslide susceptibility class area, relative error and absolute error distributions are reported.

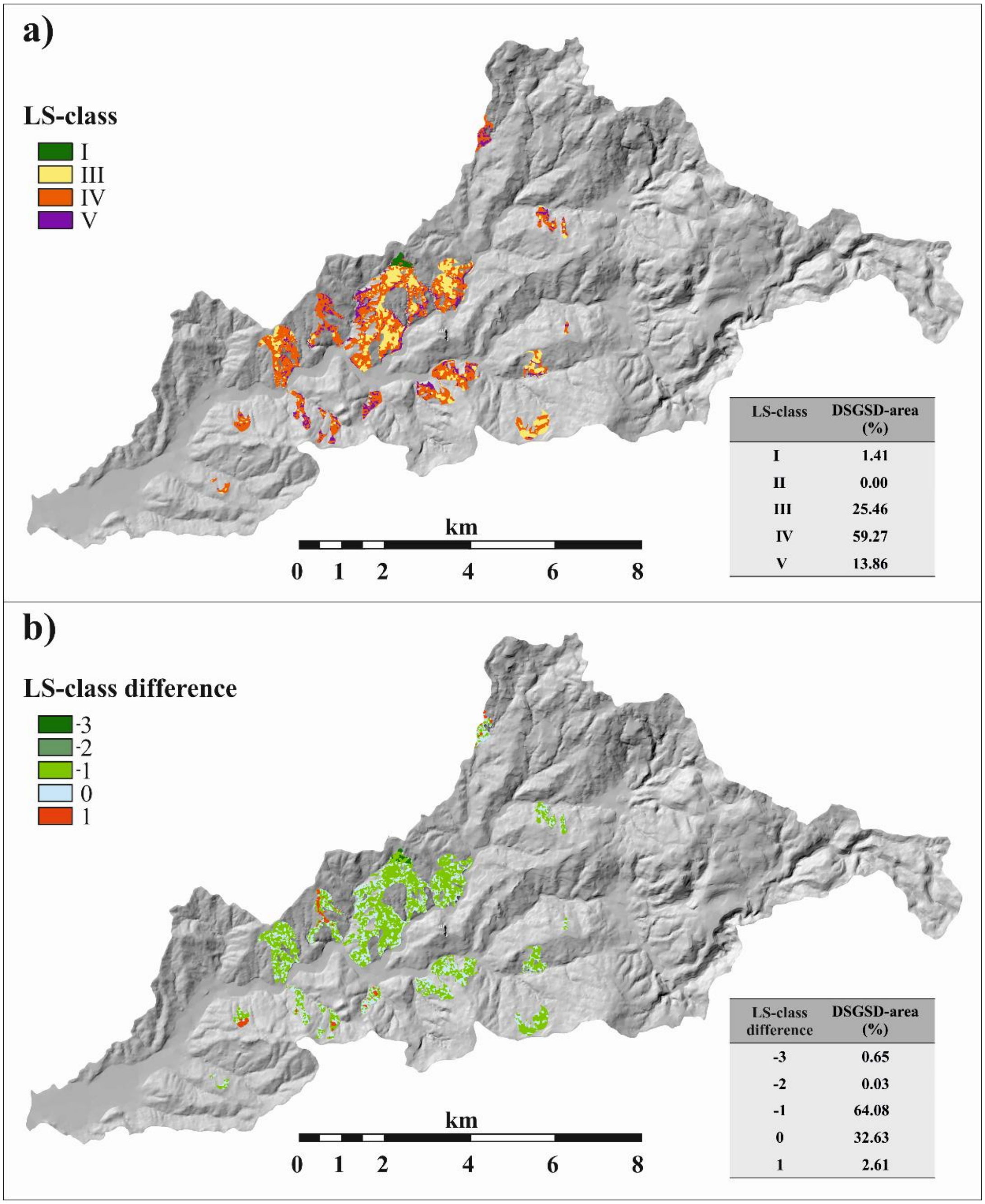

Fig. 4. The Milia LS-best model. a) Distribution of the LS over the free-landslide slopes affected by DSGSDs. b) LS-class difference between the lithology-slope angle UCUs that are affected and non-affected by DSGSDs.

Factor	Class	Class area (km^2)	MSUEs density (10^4 m^2/km^2)	Factor	Class	Class area (km^2)	MSUEs density (10^4 m^2/km^2)
Lithology (L)	Sandy Complex	5.6	0	Slope aspect (A)	]0-45°]	19.6	5.25
	Landslide body	22.4	5.11		]45-90°]	6.3	5.74
	Sandly-gravelly Complex	3.1	0.90		]90-135°]	8.6	6.08
	Gravelly Complex	9.5	9.48		]135-180°]	12.9	6.26
	Clayey-marly Complex	0.3	12.46		]180-225°]	13.7	6.39
	Shale Complex	34.5	9.18		]225-270°]	14.0	5.41
	Marly limestone flysch Complex	4.1	8.49		]270-315°]	13.6	5.43
	Sandy turbiditic Complex	1.5	3.09		]315-0°]	12.7	6.77
	Siliceous Complex	1.3	1.87	Distance to hydrographic elements (Di)	]0-50m]	26.6	3.57
	Carbonatic Complex	19.0	1.30		]50-110m]	24.8	6.93
Slope angle (S)	]0-4°]	16.5	3.01		]110-194m]	25.4	6.44
	]4-10°]	16.3	4.29		]194-793m]	24.5	6.70
	]10-12°]	18.1	6.77	Distance to tectonic lineaments (Df)	]0-102m]	24.6	6.44
	]12-15°]	16.6	7.55		]102-275m]	26.3	6.62
	]15-20°]	17.7	7.34		]275-550m]	24.4	5.79
	]20-90°]	16.1	6.03		]550-2,002m]	25.1	4.60
DSGSD (Ds)	DSGSD-presence (1)	6.2	7.96				
	DSGSD-absence (0)	95.1	5.73				

Table 1. Area and MSUEs density for each class of the factors used in the analysis.

CASE I				CASE II			
MFC	VE (%)	MD (10^4 m^2/km^2)	BMI (10^3 km^2/m^2)	MFC	VE (%)	MD (10^4 m^2/km^2)	BMI (10^3 km^2/m^2)
LS	5.2	4.28	8.24	LSDs	3.7	4.30	11.61
LSDi	5.9	4.85	8.23	LS	5.2	4.28	8.24
LDiDf	5.8	4.33	7.47	LSDi	5.9	4.85	8.23
LSDf	7.2	4.42	6.15	LSDiDs	6.9	5.27	7.63
LDi	7.5	4.30	5.73	LDiDfDs	6.0	4.51	7.52
LADi	9.7	5.12	5.28	LSDfDs	6.1	4.58	7.51
LA	8.2	4.24	5.17	LDiDf	5.8	4.33	7.47
LSA	9.6	4.77	4.97	LSDf	7.2	4.42	6.15
LSDiDf	12.5	5.15	4.12	LDi	7.5	4.30	5.73
LDf	10.8	4.02	3.72	LSADs	9.4	5.30	5.64

Table 2. The 10 best models of landslide susceptibility obtained for each case and ordered by decreasing Best Model Index (BMI) values.

Acronyms: MFC: Model Factor Combination, (L: Lithology, S: Slope angle, A: Slope aspect, Di: Distance to hydrographic elements, Df: Distance to tectonic lineaments, Ds: DSGSD-presence-absence map), VE: Validation error, MD: Mean deviation.

Lithology (L)	Slope angle (S)	DSGSD-presence (1) LS Class	DSGSD-absence (0) LS Class	UCU-LS class difference
	]0-4°]	III	III	0
	]4-10°]	IV	III	1
Gravelly	]10-12°]	IV	V	-1
Complex	]12-15°]	V	V	0
	]15-20°]	IV	V	-1
	]20-90°]	V	V	0
	]0-4°]	III	IV	-1
	]4-10°]	III	IV	-1
Shale	]10-12°]	IV	IV	0
Complex	]12-15°]	IV	V	-1
	]15-20°]	IV	V	-1
	]20-90°]	V	V	0
	]0-4°]	I	IV	-3
	]4-10°]	I	II	-1
Marly limestone	]10-12°]	I	IV	-3
flysch Complex	]12-15°]	IV	V	-1
	]15-20°]	V	V	0
	]20-90°]	III	V	-2

Table 3. The Milia LS-best model: LS-class difference between the lithology-slope angle UCUs that are affected and non-affected by DSGSDs.

Case I-LS best model	VE	X^2obs.	P (X^2< X^2obs.)
LS	5.2	0.107	< 0.05
Case II-LS best model	VE	X^2obs.	P (X^2< X^2obs.)
LSDs	3.7	0.053	< 0.01

Table 4. Chi-square statistics of the two-case best models. The chi-square test was performed with 4 degree of freedom and 0.01 confidence level (χ^2critic = 0.074).